# Magneto-transport study of intra- and intergrain transitions in the magnetic superconductors $RuSr_2GdCu_2O_8$ and $RuSr_2(Gd_{1.5}Ce_{0.5})Cu_2O_{10}$

S. García

Laboratorio de Superconductividad, Facultad de Física-IMRE, Universidad de La Habana, San Lázaro y L, Ciudad de La Habana 10400, Cuba.

J.E. Musa

Centro Brasileiro de Pesquisas Físicas, Rua Dr. Xavier Sigaud 150, Rio de Janiero, RJ 22290-180, Brazil

R.S. Freitas and L. Ghivelder

Instituto de Física, Universidade Federal do Rio de Janeiro, C.P. 68528, Rio de Janeiro , RJ 21941-972, Brazil

(Received text26 March 2003)

A characterization of the magnetic superconductors  $RuSr_2GdCu_2O_8$  [Ru-(1212)] and  $RuSr_2Gd_{1.5}Ce_{0.5}Cu_2O_{10}$  [Ru-(1222)] through resistance measurements as a function of temperature and magnetic field is presented. Two peaks in the derivative of the resistive curves are identified as intra- and intergrain superconducting transitions. Strong intragrain granularity effects are observed, and explained by considering the antiphase boundaries between structural domains of coherently rotated  $RuO_6$  octahedra as intragrain Josephson-junctions. A different field dependence of the intragrain transition temperature in these compounds was found. For Ru-(1212) it remains unchanged up to 0.1 T, decreasing for higher fields. In Ru-(1222) it smoothly diminishes with the increase in field even for a value as low as 100 Oe. These results are interpreted as a consequence of a spin-flop transition of the Ru moments. The large separation between the  $RuO_2$  layers in Ru-(1222) promotes a weak interlayer coupling, leading the magnetic transition to occur at lower fields. The suppression rate of the intragrain transition temperature is about five times higher for Ru-(1222), a result we relate to an enhancement of the 2D character of the vortex structure. A distinctive difference with conventional cuprates is the sharp increase in amplitude of the intergrain peak in both systems, as the field is raised, which is ascribed to percolation through a fraction of high quality intergrain junctions.

PACS numbers: 74.72.-h, 74.25. Fy, 74.50.+r

#### I. INTRODUCTION

The ruthenate-cuprates systems RuSr<sub>2</sub>RCu<sub>2</sub>O<sub>8</sub> [Ru-(1212)] and RuSr<sub>2</sub>(R,Ce)<sub>2</sub>Cu<sub>2</sub>O<sub>10</sub> [Ru-(1222)], where R = Gd, Eu, are currently receiving a great deal of attention. The onset of bulk superconductivity in the presence of a ferromagnetic (FM) component<sup>1,2</sup> makes these compounds particularly suitable to study the interplay between these usually exclusive phenomena. Ru-(1212) is obtained from orthorhombic  $YBa_2Cu_3O_{7-\delta}$  (YBCO) by full replacement of Cu(1) sites at the chains for Ru ions, which add two oxygen atoms to their neighborhoods in such a way that the original square coordination of Cu(1)sites evolves to RuO<sub>6</sub> octahedra and the structure becomes tetragonal.<sup>3</sup> The Ru-(1222) structure is obtained from Ru-(1212) by inserting a fluorite type  $(R_{1-x}Ce_x)_2$ block instead of the R plane.<sup>3</sup> In both Ru compounds only one distinct Cu site with fivefold pyramidal coordination exists [corresponding to the Cu(2) site in YBCO]. The result is a sequence of magnetic  $RuO_2$  planes between  $CuO_2$  superconducting bilayers. Long-range order of the Ru magnetic moments occurs at  $T_M \sim 133$  K in Ru-(1212), followed by a resistive superconducting (SC) transition at  $T_{SC} \sim 45$  K.<sup>4</sup> For Ru-(1222),  $T_M$  ranges between 125 and 155 K, depending on the Ce content,

while  $T_{SC}$  moves around 30 - 35 K.<sup>5</sup> Since in these compounds, for the first time,  $T_M >> T_{SC}$ , it has been proposed that the superconducting transition leads directly to the mixed state by spontaneous vortex phase (SVP) formation when the internal magnetization exceeds the first critical field.<sup>6,7</sup>

The detection of a sizeable Meissner signal in Ru-(1212) strongly depends on sample preparation conditions. When observed, it appears at about 15-30 K below the resistive superconducting transition. SVP formation, large magnetic penetration length and reduced effective grain size are claimed to account for this behavior.<sup>6</sup> The latter is related to the existence of intragrain domains, where the RuO<sub>6</sub> octahedra are coherently rotated around the *c*-axis, being separated by sharp antiphase boundaries.<sup>8</sup> This characteristic is also observed in Ru-(1222).<sup>9</sup>

A major open issue is how the SC state is established in a grain in the presence of a well-developed long-range magnetic order with a FM contribution. Preliminary resistivity measurements for Ru-(1212) in zero external fields suggest that a single grain behaves as a disordered Josephson-junction array (JJA).<sup>10</sup> Recent ac susceptibility experiments also support this idea.<sup>11</sup> In these reports, phase separation into antiferromagnetic (AFM) and FM domains was suggested to be the source of such behavior. However, this conjecture does not provide a consistent explanation of the magneto-transport properties, as discussed below. Instead, we propose that the Josephsonlike behavior of the intragrain transition has a structural nature in both ruthenate-cuprate systems, and that the results obtained from a careful study of the resistive SC transition in the presence of a dc magnetic field can be consistently explained with this approach.

Magnetotransport measurements are useful in order to understand the magnetic structure in the ruthenatecuprates, which is still a controversial subject, by probing how the changes in the spin order of the Ru sub-lattice are reflected in the superconducting transition. This motivated our investigation of the magnetotransport of both ruthenate-cuprate systems. In this work we present a systematic study of the resistive superconducting transition in  $RuSr_2GdCu_2O_8$  and  $RuSr_2Gd_{1.5}Ce_{0.5}Cu_2O_{10}$  in the presence of magnetic fields up to 9 T. In particular, the field dependence of the position, amplitude and width of the peaks observed in the derivative of the resistive curves is analyzed in detail. Also, ac magnetic susceptibility measurements were performed in Ru-(1212) with the same superimposed dc fields, looking for a correlation between transport and magnetic properties. For Ru-(1222), it was not possible to establish a clear correlation with ac magnetic susceptibility measurements, since this compound exhibits unique dynamic features and metastable magnetic states which complicate the interpretation.<sup>12</sup> Gd was chosen instead of Eu as the rare earth element because the phase composition of the Eubased compounds is usually slightly poorer, exhibiting a small amount of ferromagnetic SrRuO<sub>3</sub>. The paramagnetic contribution of Gd does not affect the conclusions. An YBCO sample was included in the study not only as a conventional cuprate reference, but also because of its close structural relationship with the ruthenate-cuprates. Intra- and intergrain transitions were identified and their magnetic field dependence explained in terms of the effects of the changes in the internal Ru magnetization on the antiphase boundaries, which we propose to act as weak links between structural domains. The presence of the fluorite type  $(Gd_{1,5}Ce_{0,5})$  block in Ru-(1222), which enhances the 2D character of both the vortex structure and the magnetic order in the  $RuO_2$  layers, is a relevant structural detail to explain the differences with Ru-(1212).

# **II. EXPERIMENTAL**

Polycrystalline samples of  $RuSr_2GdCu_2O_8$  and  $RuSr_2Gd_{1.5}Ce_{0.5}Cu_2O_{10}$  were prepared by conventional solid-state reaction with high purity  $RuO_2$ ,  $SrCO_3$ ,  $Gd_2O_3$ ,  $CeO_2$  and CuO powders. The initial mixtures were decomposed at 960 °C in air. After milling and pressing operations, the material was reacted in flowing nitrogen at 1000 °C for 12 hours to avoid  $SrRuO_3$  formation. Sintering was performed at 1050 °C for 4

days in flowing oxygen for Ru-(1212) and at 1060 °C for Ru-(1222), followed by cooling at a rate of 45 °C/ hour. All the samples show a density higher than 70 % the crystallographic one.

Room temperature x-ray diffraction patterns were collected to check phase composition in a Rigaku powder diffractometer in step-scanning mode  $(20^{\circ} \le 2\theta \le 80^{\circ})$ . The microstructure of the samples was probed using scanning electron microscopy (SEM). Resistance and ac susceptibility measurements were performed in a Quantum Design PPMS system, with the following dc magnetic field values: H = 0. 0.01, 0.03, 0.1, 0.3, 1, 3, 6 and 9 T, with an ac amplitude  $h_{ac} = 0.1$  Oe. The resistance was measured using a standard four-probe technique, with a polarization current of 0.1 mA. No temperature hysteresis effects were observed. The derivative of the resistive curves was obtained by conventional numerical calculations.<sup>13</sup>

# III. RESULTS

The room temperature x-ray diffraction patterns correspond to  $YBa_2Cu_3O_{7-\delta}$ ,  $RuSr_2GdCu_2O_8$  and  $RuSr_2Gd_{1.5}Ce_{0.5}Cu_2O_{10}$ , with no spurious lines being The SEM images are shown in Fig. observed. 1. For YBCO (top panel), a quite dense arrangement of parallelepiped-shaped grains with sharp edges ( $\sim 5 \times 10 \times 10$  $\mu m^3$  in size) was observed. The microstructure of Ru-(1212) shows a relatively uniform size distribution with rounded grains of about 1-3  $\mu$ m (middle panel). Some grains form compact agglomerates, which are well connected, leaving clearly distinguishable intergranular regions. For the Ru-(1222) sample (bottom panel), the microstructure exhibits a more dense packing due to the presence of a significant fraction of crystallites of  $\sim 0.5$ -1  $\mu m$  in size surrounding larger grains and filling the space between them. The larger grains are similar in average size to those observed for Ru-(1212). The small crystallites do not correspond to a secondary phase, since they are present in such extent that would become detectable in the x-ray diffraction measurements.

Figure 2 shows the temperature dependence of the resistance R(T, H) in the region of the superconducting transition for YBCO (a), Ru-(1212) (b), and Ru-(1222) (c); the values of the applied dc magnetic field are indicated. Their respective derivative curves, at constant field, are shown in Fig. 3 (note a more fine temperature scale for YBCO). Several features are relevant in the derivative curves: the number of peaks and their widths for H = 0 and the field dependence of their amplitudes, widths and positions. We first consider the reference YBCO sample. In this case, there is a sharp peak at  $T_1 = 91$  K for H = 0, with a full width-half maximum  $\Gamma$  $\sim 0.3$  K [see Fig. 3(a)]. On cooling, this peak is followed by a much broader and less intense one, located at  $T_2$ = 88.5 K. Both T<sub>1</sub> and T<sub>2</sub> are indicated by arrows in the inset of Fig. 3(a). Traditionally, the existence of two

peaks has been interpreted as intra- and intergrain SCtransitions.<sup>14</sup> In the following, we denote the high  $(T_1)$ and low  $(T_2)$  temperature maxima as intragrain and intergrain peaks, respectively. With the increase in H up to 0.3 T, peak 1 slightly moves to lower temperatures at a rate of  $\sim 0.8 \text{ K/T}$ , with a small reduction in amplitude and little increase in  $\Gamma$  ( $\Gamma \sim 0.7$  K for H = 0.3 T). For  $H \ge 1$  T, shift and broadening become more evident, but the magnitude of these effects is still  $\sim$ 1-2 K; also, a further reduction in amplitude is observed. The field dependence of the shift in  $T_1 \left[ \Delta T_1(H) = T_1(H) - T_1(0) \right]$ is shown in Fig. 4 for low fields (a) and for the whole field range (b).  $T_2$  continuously diminishes with the increase in H with an initial slope of  $\sim 20$  K/T; Fig. 5 shows the  $\Delta T_2(H) = T_2(H) - T_2(0)$  behavior. Finally, the interval between the thermodynamic transition temperature  $T_{th}$  and  $T_1$  at zero field is  $\Delta T_{th,1} = T_{th} - T_1(0) \sim 1$  K.  $T_{th}$  is taken as the value at which the derivative curve departures from the high temperature baseline, yielding  $T_{th} = 93 \pm 0.25$  K. Although  $T_{th}$  is not sharply defined due to the smooth shape of the derivative curve, there is no doubt that  $\Delta T_{th,1}$  is not greater than ~ 2 K.

For Ru-(1212) two broad overlapped peaks in the H = 0 curve were observed at temperatures T<sub>1</sub> and T<sub>2</sub>, as identified by arrows in Fig. 3(b), where T<sub>th</sub> ( $\simeq 55 \pm 1$  K) is also indicated. At first sight, this feature is absent in the Ru-(1222) sample [see Fig. 3(c)], for which an apparently single broad asymmetric peak is observed. However, the evolution of the curves with the increase in H clearly reveals the presence of two peaks. The estimation of  $\Delta$  T<sub>th,1</sub> for Ru-(1212) is ~12 K and ~17 K for Ru-(1222) (T<sub>th</sub>  $\simeq 45 \pm 1$  K), quite large in comparison to YBCO. As reported from heat capacity measurements,<sup>15</sup> T<sub>th</sub> does not diminish even for an applied field of 9 T.

The field dependence of the intragrain transition temperature  $T_1$  was found to be different in the Ru-based compounds. For Ru-(1212), the increase in H up to 0.1 T leaves peak 1 unchanged in position, width and amplitude. For  $H \ge 0.3$  T,  $T_1$  smoothly diminish with an initial slope of  $\sim 7$  K/T (one order of magnitude higher than for YBCO), while the peak strongly broadens [Fig. 3(b)]. For Ru-(1222),  $T_1$  diminishes as the field is increased even for a value as low as 100 Oe, with an initial slope of  $\sim 35$  K/T. These features are clearly evidenced in Fig. 4(a) [low field range]. For H > 0.1 – 0.3 T, the suppression rate of  $T_1$  diminishes in the ruthenate-cuprates, as can be seen in Fig. 4(b) [full range of field].

The intergrain transition temperature T<sub>2</sub> in the Rubased systems rapidly decreases for increasing fields up to H  $\simeq 0.1 - 0.3$  T, with a large initial slope of ~180 K/T. For H > 0.3 T it diminishes at a much lower rate (~0.5 K/T), as shown in Fig. 5. A relevant difference between the ruthenate-cuprate samples and YBCO is the steep increase in amplitude of peak 2, accompanied by narrowing, for H > 0.3 T [see Figs. 3 (b) and (c)].

Figure 6(a) shows the temperature dependence of the ac magnetic susceptibility  $\chi(T,H)$  for Ru-(1212), with superimposed dc magnetic fields of the same magnitude

for which the resistive curves were measured. A diamagnetic transition is very well defined for all H values at onset temperatures  $T_{o\chi}$ , which match well with the zero resistance temperatures, as determined from the resistive curves. Figure 6(b) shows an enlarged section of the region of the superconducting transition. As  $T_{o\chi}(H)$  is approached on cooling, the curves for  $H \leq 0.1$  T exhibit an upward deviation, which magnitude continuously increases with the increase in field. For  $H \geq 0.3$  T, the baseline of the curves is shifted to lower values, while the deviation continuously evolves to a smeared drop at high fields. The intragrain transitions temperatures, as determined from the peaks in the derivative of the resistive curves, are indicated by arrows for H = 6 and 9 T.

# IV. DISCUSSION

The observed suppression rates for  $T_1$  in both Rubased compounds are indicative that the intragrain superconductivity is due to a phase-lock transition of a nanoscale JJA. Additionally, we note that the shape of the  $T_1(H)$  curves in Fig. 4(b) are guite different from that expected for a bulk superconductor, i.e., from Guinzburg-Landau theory. Phase separation into nanoscale AFM and FM domains has been proposed<sup>11</sup> as a possible scenario for the Josephson-like behavior. In particular, the peak of positive magnetoresistance observed for  $\operatorname{Ru}(1212)^{16,17}$  is qualitatively explained under this assumption. However, the absence of such a peak for Ru-(1222), a system for which magnetic phase separation has also been proposed to interpret thermalmagnetic memory effects,<sup>18</sup> indicates that this interpretation is questionable. It should also be mentioned that  $\mu$ SR experiments,<sup>4</sup> which show that the internal magnetic field in the compounds is uniform, provide strong indication against the existence of magnetic domain segregation.

Alternatively, the Josephson-like behavior of the intragrain transition might be explained in terms of a phaselock process that occurs between structural domains. As already mentioned, there are domains of coherently rotated RuO<sub>6</sub> octahedra  $\sim 14^{\circ}$  around the *c*-axis, separated by sharp antiphase boundaries with local distortions in both Ru-(1212) (Ref. 8) and Ru-(1222) systems.<sup>9</sup> It has been shown that these structural domains are relevant to explain the shift to lower temperatures of the Meissner drop in Ru-(1212) in comparison to the resistive SC transition,<sup>6</sup> as a consequence of SVP formation followed by flux expulsion from the structural domains. Also, the temperature dependence of the microwave resistance for Ru-(1212) in the region of the SC transition has been consistently interpreted in terms of SVP formation.<sup>19</sup> For Ru-(1222), this mechanism has been proposed to explain the dependence of the magnetic and transport properties on the Ce concentration.<sup>20</sup> Thus, we believe that there is strong evidence to support the use of this approach to interpret our magneto-transport measurements.

The measured single-phase x-ray diffraction patterns and the SEM results allow us to rule out impurities or inhomogeneities effects as a possible cause for the the large interval between the thermodynamic and the intragrain transition temperatures,  $\Delta T_{th,1}$ , in zero external field, and therefore the results presented are essentially determined by intrinsic properties of the compounds. We interpret the large  $\Delta T_{th,1}$  values for both Ru-based compounds in zero external field in terms of SVP formation induced by the magnetization of the Ru-sub-lattice, followed by flux expulsion in the domains. For temperatures below and near  $T_{SC}$ , the vortex lines created by the internal field of the Ru sub-lattice are weakly pinned, and the Lorentz force associated to the measuring current will drive a given fraction of them. On cooling, pinning increases in the intragrain domains and flux lines are gradually trapped. Also, the first critical field of the domains increases; when it becomes higher than the internal magnetization, Meissner effect occurs in the domains, with partial expulsion of the vortex lines, leading to flux compression at the antiphase boundaries. The value of the local field at the boundaries depends on the size of the neighboring domains and the amount of flux trapped. The result is a complex thread of magnetic field lines across the intragrain network, generating a variety of local effective fields. If the boundaries act as Josephson junctions, the domains will gradually become phaselocked as the temperature is decreased, until a maximum rate of the percolation process is reached at  $T_1$ . The higher  $\Delta T_{th,1}$  by about 5 K for Ru-(1222) is attributed to the larger distance between the  $CuO_2$  planes. This structural feature enhances the 2D character of the vortex lattice, promoting a less pinned structure. Lower temperatures will be required to prevent dissipation associated to flux motion and to achieve a stationary flux distribution at the interdomain boundaries, through which the intragrain percolation may proceed. These effects in zero external field are absent for YBCO, since there is neither SVP formation nor a domain structure.

#### A. Intragrain transition in Ru-(1212)

In the scheme depicted above the magnetization of the Ru sub-lattice is essential in determining the details of the spontaneous vortex structure. The fact that  $T_1$  remains unchanged for Ru-(1212) up to H = 0.1 T suggests that a) an external field of this strength has a little effect on the magnetization of the RuO<sub>2</sub> layers at temperatures around 40-50 K (~90 K below  $T_M$ ), and b) the effective internal field at the boundaries is considerably higher than the applied magnetic field. At first sight, point b) seems to be in contradiction with the fact that internal fields of only ~700 Oe have been measured at the Gd site by electronic paramagnetic resonance (EPR)<sup>21</sup> and at the so called apical site of the structure by  $\mu$ SR measurements.<sup>4</sup> However, when the Meissner effect is established in the structural domains, a number of vortex

lines are expulsed from them and compressed into the thin thickness of the antiphase boundaries, leading to a high local field. This is the actual value of field through which a coherent SC state has to nucleate between domains. External fields  $H \leq 0.1$  T make a negligible contribution to the interdomain field, and no shift in the intragrain peak is observed.

The effect of an external field on the intragrain transition is important for promoting a re-arrangement in the magnetic order of the Ru moments. The fact that the  $\chi(T,H)$  curves change their behavior just at  $H \simeq 0.1$  -0.3 T, supports this idea. We recall that for Ru-(1212) when a magnetic field H = 0.4 T is applied a change in the neutron diffraction pattern is observed, a result interpreted as due to a spin-flop transition.<sup>22</sup> Also, detailed magnetic measurements in this compound indicate that a spin-flop transition should occur at a critical field of ~0.14 T for crystallites with the RuO<sub>2</sub> layers oriented parallel to the applied field.<sup>23</sup> These values are near to the fields at which we observed the decrease in T<sub>1</sub> and the changes in the  $\chi(T, H)$  curves.

The features observed in the  $\chi(T, H)$  curves can also be explained in terms of a spin transition. The evolution from an upward deviation to a drop as the field is increased beyond 0.1 T implies that the relative contribution to the net magnetization from components of different sign changes. The main two contributions to the positive background are the FM component of the Ru sub-lattice and the paramagnetic signal of the Gd moments. The fact that the diamagnetic contribution becomes gradually detectable for  $H \gtrsim 0.1$  T suggests that the FM component is reduced as a consequence of the spin re-orientation, possibly including a change of the Ru moments from *c*-axis alignment to planar, as proposed from neutron diffraction measurements.<sup>22</sup> According to this assumption, the magnetization at the  $CuO_2$  superconducting planes will be lowered, leading either to a mixed state with a lower density of vortex lines, i.e., with an increased fraction of the superconducting volume, or preventing SVP formation if the internal magnetization becomes lower than the first critical field of the domains. The boundaries will then be under the action of higher flux compression, as it is expulsed in a larger extent. If the intragrain transition is considered to be a phase-lock transition between structural domains, lower temperatures will be required to achieve intragrain percolation through a network of boundaries with an increased average local field. Also, under this approach, the number of screened Gd paramagnetic ions will be increased. Thus, the picture of a magnetic transition leading to a state with a reduced Ru magnetization diminishes the positive components to the net magnetization, increases the superconducting fraction in the domains, and depletes the intragrain transition temperature. It is worth mentioning that this analysis is independent of the actual order of the Ru moments below the spin-flop transition, and additional microscopic results are needed to interpret our magnetotransport measurements in terms of a well defined magnetic structure.

#### B. Intragrain transition in Ru-(1222)

The decrease of  $T_1$  in Ru-(1222) for a field as low as 100 Oe, as shown in Fig. 4(a), suggests a different magnetic response of the Ru sub-lattice in this compound. We believe that the enhancement of the 2D character of the magnetic order of the  $RuO_2$  layers due to the insertion of the  $(Gd, Ce)_2O_2$  fluorite block instead of the Gd plane in Ru-(1212), is a key point to understand this behavior. The larger separation between the magnetic layers in Ru-(1222) leads to a weak superexchange coupling between the layers. In addition, differently than the case of Ru-(1212), any possible chains would be also affected by the fact that the nearest-neighbor Ru ions are not vertically aligned due to a shift induced by the fluorite block. Thus, other mechanisms are needed to attain a long-range order of the Ru moments along the *c*-axis. Recently, an interlayer coupling via dipole-dipole interaction has been proposed to explain the hysteretic behavior of Ru-(1222), leading to a spin-flop of the Ru moments for magnetic fields in the 0-100 Oe range,<sup>12</sup> a result which agrees with our interpretation. In addition, magnetic frustration effects and spin-glass behavior have been claimed to explain magnetic relaxation results in Ru-(1222), consistently with a weak magnetic coupling in this system.<sup>24</sup>

There is yet another important difference between the Ru-(1212) and Ru-(1222) systems in relation to the magnetism of the  $RuO_2$  layers which favors  $T_1$  suppression at low fields in the latter compound. For Ru-(1222), XANES measurements<sup>25</sup> reveal the absence of a  $Ru^{4+}/Ru^{5+}$  mixed valence state, as observed in Ru-(1212).<sup>26</sup> This precludes the emergence of ferrimagnetic order in Ru-(1222). Ferrimagnetism in Ru-(1212) has been claimed to be the source of the high magnetization measured for this compound,<sup>23</sup> which can not be explained only in terms of spin canting considerations. These results are relevant to the present study because they point to a state of low internal magnetization in Ru-(1222) at zero external field. Unfortunately, the long-range order of the Ru moments in Ru-(1222) is unknown; although neutron powder diffraction results were reported,<sup>9</sup> the exact magnetic structure has not been unveiled.

The approximately five times larger suppression rate of  $T_1 (\sim 35 \text{ K/T})$  at low fields in comparison to Ru-(1212) can be understood upon the same considerations used to explain the larger  $\Delta T_{th,1}$  interval in Ru-(1222). As the external field is increased, the vortex structure in Ru-(1222), which has a higher 2D character, will be depinned more easily. Further cooling in comparison to Ru-(1212) would be required to attain a stable configuration of flux lines across the interdomain boundaries, shifting the intragrain transition to lower temperatures.

# C. Intergrain transitions

Both compounds exhibit a rapid decrease of the intergrain transition temperature T<sub>2</sub>, for H  $\leq 0.1$ - 0.3 T, with an initial slope which is one order of magnitude higher than for YBCO, followed by a much smaller suppression rate at higher fields (see Fig. 5). For Ru-(1212) it is possible to establish a clear correlation between the  $T_2(H)$ behavior and the field dependence of  $T_1$ . Since there are no changes in the intragrain transition up to H = 0.1 T, the contribution of the Ru magnetization in the grains to an effective field at the intergrain links remains essentially the same. Thus, the decrease in  $T_2$  in this interval is only due to the increase in the external field. For H >0.1 T, the magnetic transition towards the proposed state of lower internal magnetization gradually takes place in the polycrystalline sample with the increase in field. This reduces the contribution of a fraction of the grains to the local field at their neighboring intergrain junctions. The net effect of an increasing external field acting on an intergrain network which improves its connectivity as the intragrain magnetic transition proceeds is a lower suppression rate in  $T_2$ . For Ru-(1222) the interpretation is less clear, since in this case there is not a well defined magnetic field value at which the re-arrangement of the Ru moments occurs, but instead a smooth decrease of  $T_1$ . However, whatever the exact order of the Ru moments at low fields in this system might be, the  $T_1(H)$ curve also shows a rapid variation in the H  $\simeq$  0.1- 0.3 T interval, followed by a lower suppression rate [see Fig. 4(b)].

The field dependence of the amplitude of the intergrain peak in the Ru-based compounds has a distinctive difference as compared with YBCO. Although it regularly diminishes with the increase in field up to H =0.1 T, accompanied with broadening, as in the conventional cuprates, a steep increase and narrowing are observed for H > 0.3 T. In YBCO, the intergrain transition occurs over a wide distribution of link qualities, which become gradually phase-locked on cooling, leading to a broad peak. One possible explanation for the ruthenatecuprates behavior in the high field range is that low quality links would be inactivated definitively due to the contribution of the magnetization in the grains to the effective field at the junctions. In this scheme, the intergrain transition would take place only through a fraction of high quality connections. This fraction of "available" links diminishes as the external field is increased, and so the range of temperatures in which percolation proceeds, leading to sharper transitions.

Another interesting feature of the field dependence of the intergrain transition is that the  $T_2(H)$  curves, including YBCO, have a very similar slope for H > 0.3 T, as can be seen in Fig. 5, suggesting that the curves are displaced due to the contribution of the magnetization in the grains to the effective field at the intergrain links. The fact that for Ru-(1222) the reduction of  $T_2$  for a given field is smaller than for Ru-(1212) is consistent with our previous considerations about a lower magnetization in the grains for the former compound. Additional studies are needed for a better understanding of the role of the grain magnetization in the intergrain transition.

# V. CONCLUSIONS

We presented data indicating that the intragrain transition in both Ru-(1212) and Ru-(1222) exhibits a phaselock behavior of a nanoscale Josephson-junction array. It is proposed that the presence of domains of coherently rotated RuO<sub>6</sub> octahedra, a common structural feature of both compounds, is the source of such behavior. The differences in the field dependence of the intragrain transitions in these systems are interpret in terms of the magnetic response of the  $RuO_2$  layers. The addition of the  $(Gd, Ce)_2$  block in Ru-(1222) is a key point to explain why a spin-flop transition occurs in this material at a field one order of magnitude lower than for Ru-(1212), due to the enhancement of the 2D character of the magnetic order in the  $RuO_2$  layers. We argue also that this structural difference promotes a less pinned vortex lattice, leading to a five times larger suppression rate in the intragrain transition at low fields. The field dependence of the intergrain transition temperature is consistent with the changes in the intragrain magnetization in both compounds. The sharp intergrain peak at high fields suggests that intergrain percolation occurs only through a fraction of high quality junctions.

# Acknowledgments

S. García acknowledges financial support from FAPERJ, CAPES-Brazil, and CLAF (Latin American Centre of Physics). R.S. Freitas was supported by FAPERJ. We thank A. López and R. Cobas for help in sample preparation, and E.M. Baggio-Saitovitch for fruitful discussions.

# VI. FIGURE CAPTIONS

Figure. 1. Scanning electron microscopy images of  $YBa_2Cu_3O_7$  (YBCO - top panel);  $RuSr_2GdCu_2O_8$  (Ru-[1212] - middle panel); and  $RuSr_2Gd_{1.5}Ce_{0.5}Cu_2O_{10}$  (Ru-[1222] - bottom panel).

Fig. 2. Temperature dependence of the resistance, measured with dc magnetic fields H = 0, 0.01, 0.03, 0.1, 0.3, 1, 3, 6, and 9 T: (a) YBCO, (b) Ru-(1212) and (c) Ru-(1222).

Fig. 3. Derivative dR/dT of the resistive curves shown in Fig. 1: (a) YBCO, (b) Ru-(1212) and (c) Ru-(1222). Inset in (a): an enlarged region of the derivative curve for YBCO at zero external field. The intragrain (T<sub>1</sub>) and intergrain (T<sub>2</sub>) peaks are identified in the inset and in panel (b) for H = 0 T. The thermodynamic transition temperature T<sub>th</sub> is indicated for Ru-(1212). The lines are guides to the eyes.

Fig. 4. Field dependence of the shift in the intragrain transition temperature,  $\Delta T_1(H) = T_1(H) - T_1(0)$ , as determined from the derivative of the resistive curves of the studied samples: (a) an enlarged section of the low field interval, and (b) for the whole range of fields. The lines are guides to the eyes.

Fig. 5. Field dependence of the shift in the intergrain transition temperature,  $\Delta T_2(H) = T_2(H) - T_2(0)$ , as determined from the derivative of the resistive curves. The lines are guides to the eyes.

Fig. 6 (a) Temperature dependence of the ac magnetic susceptibility for Ru-(1212). The dc magnetic fields are the same used in the resistance measurements; (b) an enlarged section of the region of the superconducting transition. For H = 6 and 9 T the temperatures at which the corresponding intragrain peaks occur in the derivative of the resistive curves are indicated by arrows. The lines are guides to the eyes.

- <sup>1</sup> I. Felner, U. Asaf, Y. Levi, and O. Millo, Phys. Rev B 55, R3374 (1997).
- <sup>2</sup> J.L. Tallon, C. Bernhard, M.E. Bowden, P.W. Gilberd, T.M. Stoto, and Pringle, IEEE Trans. Appl. Supercond. 9, 1696 (1999).
- <sup>3</sup> R. J. Cava, J. J. Krajewsky, H. Takagi, H. W. Zandbergen, R. B. Van Dover, W. F. Peck Jr., and B. Hessen, Physica C **191**, 237 (1992).
- <sup>4</sup> C. Bernhard, J. L. Tallon, Ch. Niedermayer, Th. Blasius, A. Golnik, E. Brücher, R. K. Kremer, D. R. Noakes, C. E. Stronach, and E. J. Ansaldo, Phys. Rev B **59**, 14099 (1999).
- <sup>5</sup> I. Felner, U. Asaf, and E. Galstyan, Phys. Rev B 66, 024503 (2002).

- <sup>6</sup> C. Bernhard, J. L. Tallon, E. Brücher, and R. K. Kremer, Phys. Rev B **61**, R14960 (2000).
- <sup>7</sup> E.B. Sonin, and I. Felner, Phys. Rev. B **57**, 14000 (1998).
- <sup>8</sup> A. C. McLaughlin, W. Zhou, J. P. Attfield, A. N. Fitch, and J. L. Tallon, Phys. Rev B **60**, 7512 (1999).
- <sup>9</sup> C.S. Knee, B.D. Rainford, and M.T. Weller, J. Mater. Chem. **10**, 2445 (2000).
- <sup>10</sup> Y.Y. Xue, B. Lorenz, R.L. Meng, A. Baikalove, and C.W. Chu, Physica C **364-365**, 251 (2001).
- <sup>11</sup> B. Lorenz, Y.Y. Xue, R.L. Meng, and C.W. Chu, Phys. Rev B **65**, 174503 (2002).
- <sup>12</sup> I. Živković, Y. Hirai, B.H. Frazer, M. Prester, D. Drobac, D. Ariosa, H. Berger, D. Pavuna, G. Margaritondo, I. Felner, and M. Onellion, Phys. Rev. B **65**, 144420 (2002).

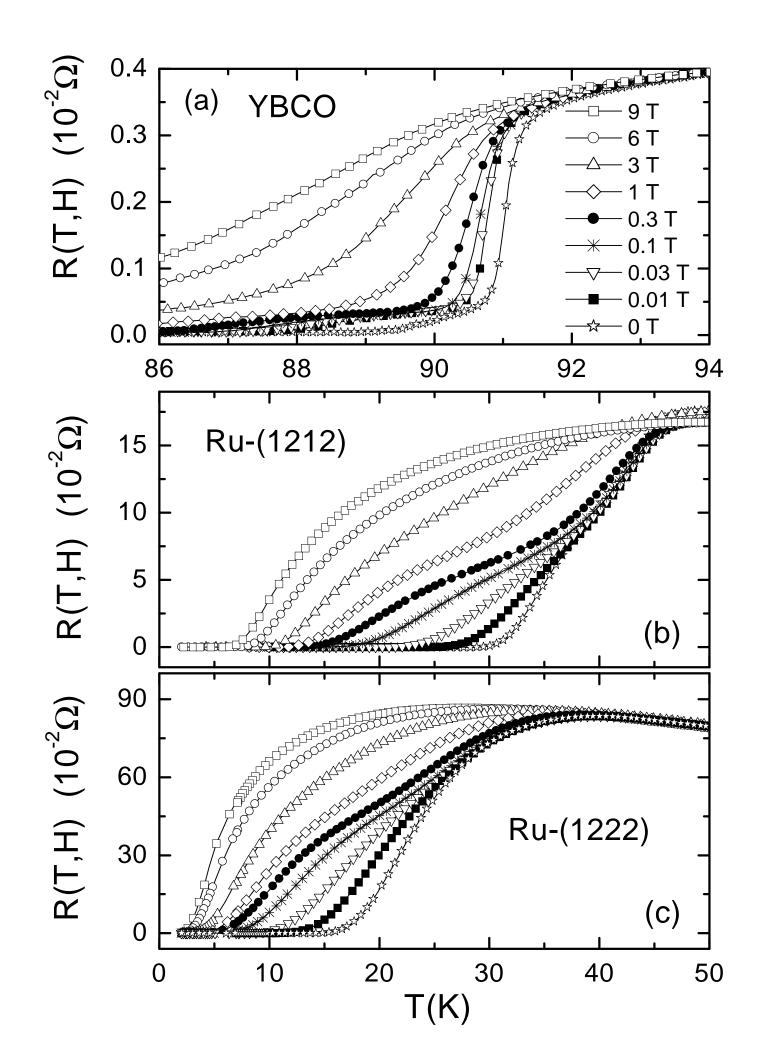
- <sup>13</sup> P. Pureur and J. Schaf, J. Magn. Magn. Mater. **69**, L-215 (1987).
- <sup>14</sup> E.A. Éarly, C. C. Almasan, R. F. Jardim, and M. B. Maple, Phys. Rev. B **47**, 433 (1993).
- <sup>15</sup> J.L. Tallon, J.W. Loram, G.V.M. Williams, and C. Bernhard, Phys. Rev B **61**, R6471 (2000).
- <sup>16</sup> J.E. McCrone, J. R. Cooper, and J.L. Tallon, J. Low Temp. Phys. **117**, 1199, (1999).
- <sup>17</sup> X.H. Chen, Z. Sun, K.Q. Wang, S.Y. Li, Y.M. Xiong, M. Yu, and L.Z. Cao, Phys. Rev. B **63**, 064506 (2001).
- <sup>18</sup> Y.Y. Xue, D.H. Cao, B. Lorenz, and C.W. Chu, Phys. Rev B **65**, 020511(R) (2001).
- <sup>19</sup> M. Požek, A. Dulčic, D. Paar, G.V.M. Williams, and S. Krämer, Phys. Rev. B **64**, 064508 (2001).
- <sup>20</sup> G.V.M. Williams, L.-Y. Jang, and R.S. Liu, Phys. Rev. B

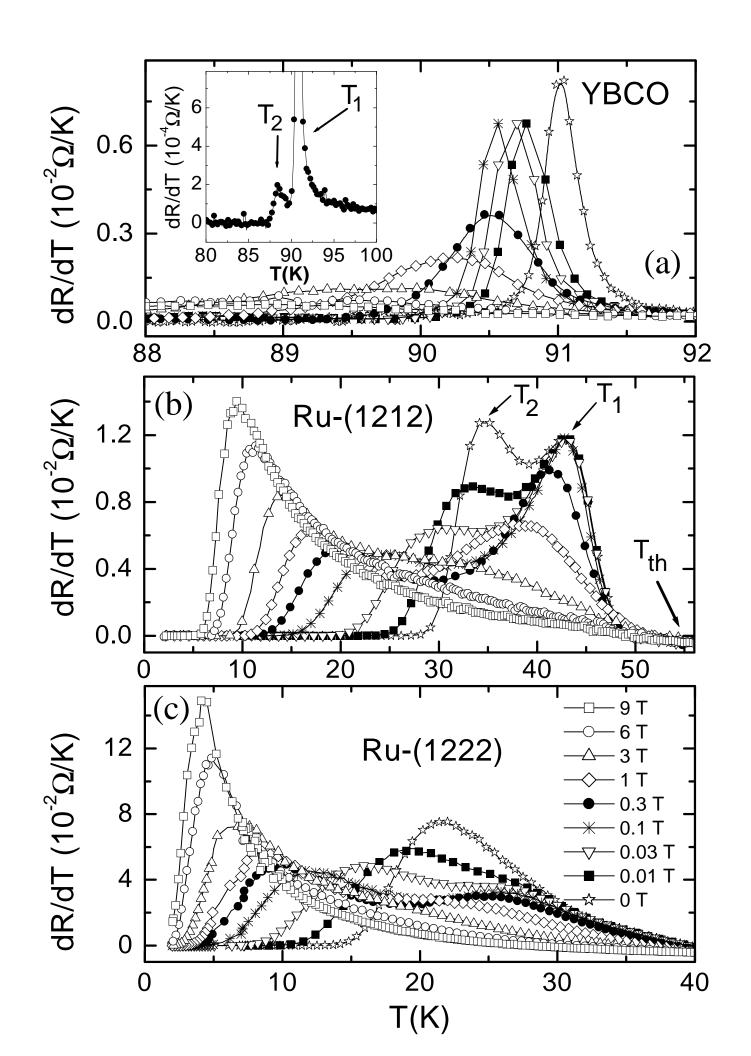
B 65, 064508 (2002).

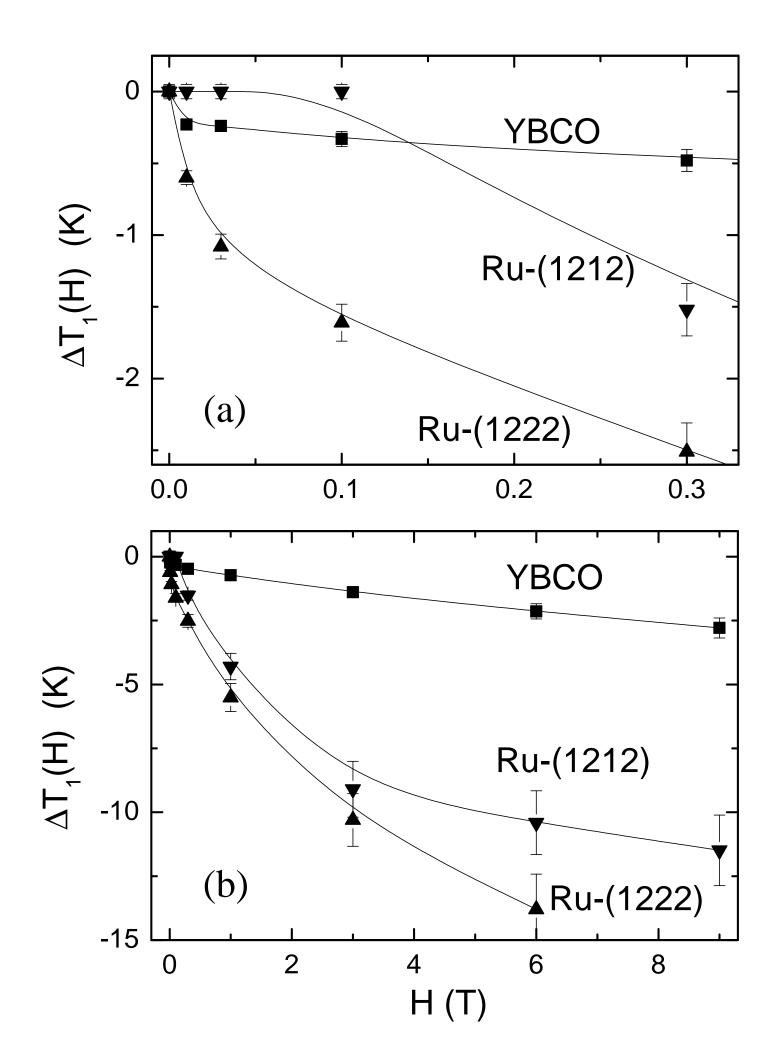
- <sup>21</sup> A. Fainstein, E. Winkler, A. Butera, and J. Tallon, Phys. Rev B **60**, R12597 (1999).
- <sup>22</sup> J. W. Lynn, B. Keimer, C. Ulrich, C. Bernhard, and J.L. Tallon, Phys. Rev B **61**, R14964 (2000).
- <sup>23</sup> A. Butera, A. Fainstein, E. Winkler, and J. Tallon, Phys. Rev. B **63**, 054442 (2001).
- <sup>24</sup> C.A. Cardoso, F.M. Araújo-Moreira, V.P.S. Awana, E. Takayama-Muromachi, O.F. de Lima, H. Yamauchi, and M. Karppinen, Phys. Rev. B 67, 020407 (2003).
- <sup>25</sup> I. Felner, U. Asaf, C. Godart, and E. Alleno, Physica B 259-261, 703 (1999).
- <sup>26</sup> R. S. Liu, L. Y. Jang, H. H. Hung, and J. L. Tallon, Phys. Rev B **63**, 212507 (2001).

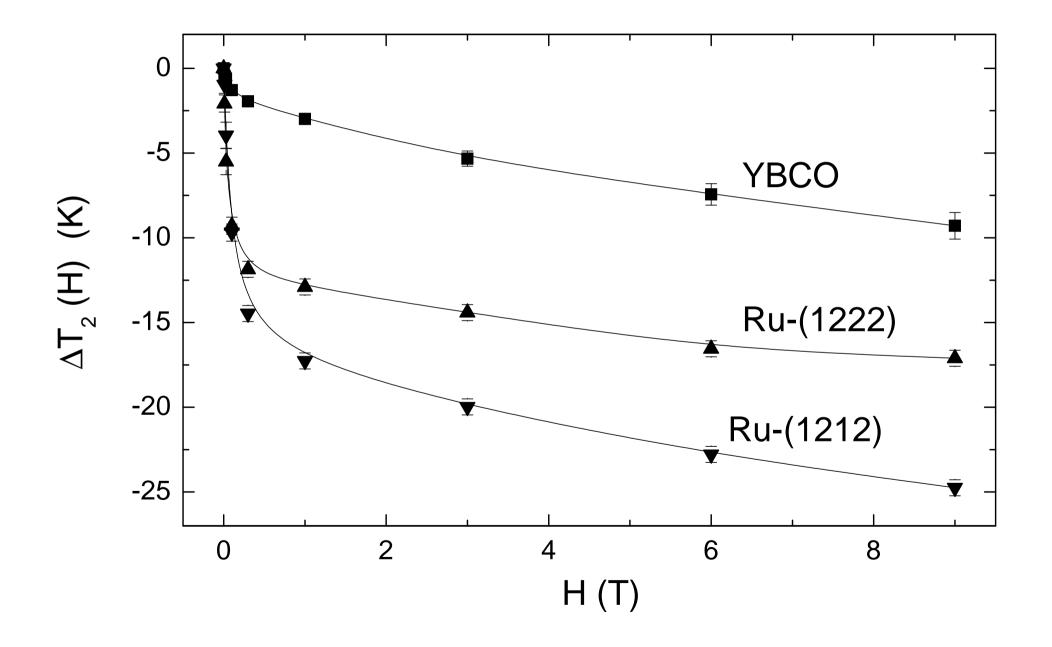
This figure "Fig1.jpg" is available in "jpg" format from:

http://arxiv.org/ps/cond-mat/0306228v1









 $\chi$  (T, H) (10<sup>-2</sup>emu/Oe.g)

